PART VI

Coastal, Estuarine and Environmental Problems

Porto Cala Galera, Toscana

Ventotene Island, Lazio

CHAPTER 207

INTERACTION BETWEEN
WATER WAVES AND VEGETATION

by

Toshiyuki Asano [1]
Hiroshi Deguchi [2]
and
Nobuhisa Kobayashi [3]

1.INTRODUCTION

The presence of densely growing vegetation has been observed to result in wave damping and shoreline sediment deposition. Submerged or flooded vegetation, seaweed stands, reed stands and mangrove forests act as a buffer zone against wave attack on the rear beaches. Recently, a new method for shoreline protection by use of artificial seaweed has been attempted(Rogers 1986; Jenkins and Skelly 1987).

Besides the function of shoreline protection, these vegetated areas play an important role in estuarine and nearshore ecosystems. Since the hydrodynamic process is one of the most important governing factors of the ecosystems, the interaction between water waves and vegetation needs to be quantified. Furthermore, the need of improved understanding of this mechanisms may increase since accelerated sea level rise may result in more flooding in vegetated areas(ASCE Task Committee 1992)

One of the authors initiated a study by conducting experiments on wave damping using artificial seaweed(Asano et al. 1988). Recently, an analytical model was developed to describe the vertically two-dimensional problem of small amplitude waves propagating over submerged or subaerial vegetation

[1]Dept. of Ocean Civil Engrg., Kagoshima Univ., Korimoto, Kagoshima, 890, JAPAN
[2]Sekisui-House Inc., Kintetsu Dojima Bild., Dojima 2-2-2, Osaka, 530, JAPAN
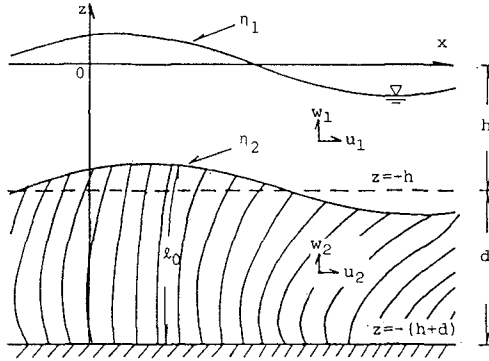[3]Dept. of Civil Engrg., Univ. of Delaware, Newark, DE, 19716, U.S.A.

Figure 1: Definition sketch of two layer model

(Kobayashi, Reichle and Asano 1992). This analytical model is referred to as the previous model in this paper.

In the previous model, the effect of vegetation on the flow field was assumed to be expressible in terms of the drag resistance against the fluid motion, whereas the decrease in the drag resistance due to the swaying motion of vegetation was neglected. An analytical solution was obtained for the monochromatic waves whose height decayed exponentially. The comparisons with the artificial seaweed experiments yielded the calibrated drag coefficients C_D varying in a wide range and affected by the vegetation motion. The calibrated values of C_D were on the order of 0.1 for the tests with swaying vegetation. A greater value of C_D would have been resulted if the relative velocity between the fluid and vegetation motion had been used for the drag resistance.

The present paper extends the previous model by including the interaction between the wave and vegetation motion. The present model consists of analyses for the flow field and the swaying motion of an individual vegetation stand. Both solutions are connected by a linearized damping coefficient D which is determined iteratively. The interaction effects are hence included in the converged solution. The calculated results are compared with the artificial seaweed experiments. The measured wave attenuation is reproduced well by the extended model using a drag coefficient of the order of unity.

2. SOLUTION FOR FLOW FIELD

A two-layer model consisting of an upper fluid layer of depth h, and a lower fluid layer of depth d, is shown in Fig. 1. The depth d of the lower layer is the mean height of swaying vegetation and is less than the vegetation length

l_0. In this linearized analysis, small-amplitude monochromatic waves are assumed to propagate in the positive direction of the horizontal coordinate x and be attenuated by the vegetation. The vertical coordinate z is taken to be positive upward with $z = 0$ at the still water level (SWL). Viscous shear stresses acting on the interface and the bottom are neglected because the drag resistance of the vegetation is predominant for most practical applications.

The linearized momentum equations in the upper and lower layers, which are indicated by the subscripts 1 and 2, respectively, may be expressed as

$$\frac{\partial \mathbf{u_1}}{\partial t} = -\frac{1}{\rho}\nabla p_1 \tag{1}$$

$$\frac{\partial \mathbf{u_2}}{\partial t} = -\frac{1}{\rho}\nabla p_2 - \frac{1}{\rho}\mathbf{F} \tag{2}$$

in which, t = time; $\mathbf{u} = (\mathbf{u}, \mathbf{w})$ = water particle velocity vector; ρ = fluid density; and p = dynamic water pressure due to waves.

The drag force vector per unit volume, $\mathbf{F}$, in (2) is assumed to be given by

$$F_x = \tfrac{1}{2}\rho C_D b N u_r \mid u_r \mid,$$
$$F_z = 0 \tag{3}$$

in which C_D = drag coefficient; b = area per unit height of each vegetation stand normal to the horizontal velocity; N = number of vegetation stands per unit horizontal area; and $u_r = (u_2 - u_v)$ is the relative velocity between the horizontal fluid velocity u_2 and the swaying velocity of vegetation, u_v. The drag force is assumed to be dominant and the inertia force is neglected in (3).

In order to derive an analytical solution, (3) is linearized as follows:

$$\frac{1}{2}\rho C_D b N u_r \mid u_r \mid = \rho D u_2 \tag{4}$$

The damping coefficient D is determined in such a way that the mean square of the error, $\overline{E_r^2}$, of the difference between both sides of (4) is the minimum. The condition of $\partial \overline{E_r^2}/\partial D = 0$ gives

$$D = \frac{1}{2}C_D b N \; \frac{\overline{\displaystyle\int_{-(h+d)}^{-h} u_r \mid u_r \mid u_2 \, dz}}{\overline{\displaystyle\int_{-(h+d)}^{-h} u_2^2 dz}} \tag{5}$$

The unknown coefficient D depends on u_2 and u_r and will be determined by iterations using the solutions for u_2 and u_v as will be explained later.

Eq.(2) can then be linearized as

$$\frac{\partial u_2}{\partial t} = -\frac{1}{\rho}\frac{\partial p_2}{\partial x} - Du_2,$$

$$\frac{\partial w_2}{\partial t} = -\frac{1}{\rho}\frac{\partial p_2}{\partial z} \tag{6}$$

The momentum equations (1) and (6) as well as the continuity equations for both upper and lower layers are subject to the following linearized boundary conditions at the free surface, interface and bottom boundaries:

$$\frac{\partial \eta_1}{\partial t} = w_1, \qquad p_1 = \rho g \eta_1 \qquad at \;\; z = 0,$$

$$\frac{\partial \eta_2}{\partial t} = w_1 = w_2, \qquad p_1 = p_2, \qquad at \;\; z = -h,$$

$$w_2 = 0 \qquad\qquad\qquad at \;\; z = -(h+d) \tag{7}$$

where η_1 = free surface elevation above SWL; η_2 = displacement of the interface; and g = gravitational acceleration.

In the following, η_1 is assumed to be expressible in a sinusoidal form with a complex wave number $k = (k_r + i k_i)$ as follows:

$$\eta_1 = a_0 \exp\{i(kx - \sigma t)\} \tag{8}$$

in which, $i^2 = -1$; a_0 = wave amplitude at x=0; and σ = angular frequency. From the real part of (8), the local wave amplitude is found to decay exponentially

$$a = a_0 \exp(-k_i x) \tag{9}$$

where k_i = exponential decay coefficient.

The solutions for the horizontal fluid velocities u_1 and u_2 can be shown to be given by

$$u_1 = \frac{gka_0}{\sigma}\{\cosh(kz) + \frac{\sigma^2}{gk}\sinh(kz)\}\exp\{i(kx - \sigma t)\} \tag{10}$$

$$u_2 = \frac{g\alpha^2 a_0}{\sigma k}\{\cosh(kh) - \frac{\sigma^2}{gk}\sinh(kh)\}\frac{\cosh[\alpha(z + h + d)]}{\cosh(\alpha d)}\exp\{i(kx - \sigma t)\} \tag{11}$$

with

$$\alpha = k/\sqrt{1 + i(D/\sigma)} \tag{12}$$

Substituting (10) and (11) into (1) and (6) yields the solutions for the pressures p_1 and p_2

$$p_1 = \frac{\rho\sigma}{k}u_1$$

$$p_2 = \frac{\rho(\sigma + iD)}{k}u_2 \tag{13}$$

The continuity equations together with (10) and (11) yield the solutions for the vertical fluid velocities w_1 and w_2, which are omitted herein.

Furthermore, the vertical displacement of the interface, η_2, is given by

$$\eta_2 = a_0[\cosh(kh) - \frac{gk}{\sigma^2}\sinh(kh)]\exp\{i(kx - \sigma t)\} \tag{14}$$

Lastly, the dispersion relation is given by

$$\sigma^2 = gk\frac{k\tanh(kh) + \alpha\tanh(\alpha d)}{k + \alpha\tanh(\alpha d)\tanh(kh)} \tag{15}$$

Eq. (15) can be solved to find the unknown complex wave number k for given σ, h, d, g and D.

In the case of weak damping $\sigma \gg D$, (15) can be expressed more explicitly. Eq.(12) is simplified as

$$\alpha \simeq k(1 - i\frac{D}{\sigma})^{1/2} \simeq k(1 - i\frac{D}{2\sigma}) \tag{16}$$

Since $\alpha = [k(1 - i\epsilon) + O(\epsilon^2)]$ with $\epsilon = D/2\sigma$, (15) becomes

$$\sigma^2 = gk\tanh[k(h + d)]\left[1 - i\epsilon\frac{2kd + \sinh(2kd)}{\sinh[2k(h + d)]}\right] \tag{17}$$

The real and imaginary parts of (17) yield the following equations

$$\sigma^2 = gk_r\tanh[k_r(h + d)] \tag{18}$$

$$\frac{k_i}{k_r} = \epsilon\frac{2k_r d + \sinh(2k_r d)}{2k_r(h + d) + \sinh[2k_r(h + d)]} \tag{19}$$

Eq.(18) is the ordinal dispersion relation for small-amplitude water waves, so the presence of vegetation does not change the real wave number k_r as long as $\epsilon = (D/2\sigma)$ is much smaller than unity. On the other hand, (19) implies that $k_i/k_r = \mathbf{O}(\epsilon)$

The above analytical solution for the flow field is the same as that obtained by Kobayashi et al. (1992) except that D was given by (5) with $u_r = (u_2 - u_v)$ replaced by u_2.

3. SOLUTION FOR VEGETATION MOTION

The behaviour of a vegetation colony under wave action is complex because the vegetation and fluid motions may generate turbulence stresses along the interfacial boundary and among the vegetation stands. However, it is observed that each stand does not move in random but a group of stands sway
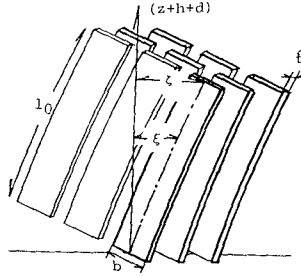
Figure 2: Model of vegetation motion

in an organized manner. As long as the vegetation motion is not so large, it may be treated as a horizontal swaying motion as shown in Fig.2.

As a first attempt, the vegetation motion due to wave action is simply modelled as a forced vibration with one degree of freedom. The buoyancy and stiffness of the vegetation material are considered as the restoring forces of the vibration. The horizontal displacement of a vegetation stand from the vertical z-axis is denoted by ξ, while the differentiations with respect to t and z are indicated by the over dot and the subscript z, respectively. The equation of the motion for each stand may be expressed as follows:

$$\rho_v b \hat{t} \ddot{\xi} + C_1 \dot{\xi} + EI \xi_{zzzz} = \tfrac{1}{2}\rho C_D b \mid u_2 - \dot{\xi} \mid (u_2 - \dot{\xi})$$
$$+\rho(C_M - 1)b\hat{t}(\dot{u}_2 - \ddot{\xi}) + \rho b \hat{t} \dot{u}_2 - (\rho - \rho_v)gb\hat{t}\xi_z \qquad (20)$$

in which $\rho_v, b, \hat{t}, EI, C_1$ and C_M are the density, width, thickness, bending stiffness, attenuation constant, inertia coefficient of the vegetation strip , respectively. It is noted that $\dot{\xi} = u_v$ and $u_r = (u_2 - \dot{\xi})$ in (5). The inertia force is included on the right hand side of (20) for completedness, although it is neglected in (3). Assuming that $C_1 = 0$, $(\dot{\xi}/u) \ll 1$ and ξ may be approximated by $\xi = \{(z + h + d)/d\}\zeta$ with ζ being the horizontal displacement at the top of the vegetation strip, (20) may be simplified as follows:

$$\tfrac{1}{2}\{\rho(C_M - 1) + \rho_v\}V\ddot{\zeta} + \tfrac{1}{2}\rho C_D \mid u \mid A\dot{\zeta} + \{\frac{8EI}{d^3} + (\rho - \rho_v)g\frac{V}{d}\}\zeta$$
$$= \tfrac{1}{2}\rho C_D A u \mid u \mid +\rho C_M V \dot{u} \qquad (21)$$

in which $A = bd$ and $V = bd\hat{t}$. In the derivation of (21), it is assumed

$$\int_{-(h+d)}^{-d} EI \xi_{zzzz} dz = \frac{8EI}{d^3}\zeta \qquad (22)$$

which is the relation for the displacement at the top of a cantilever under uniform loading. In addition, u, $\dot{u}$ and $\mid u \mid u$ in (21) should be taken as the depth-averaged values of u_2, $\dot{u}_2$ and $\mid u_2 \mid u_2$ in the region $-h \geq z \geq -(h+d)$.

4. WAVE DAMPING CHARACTERISTICS

(1)Interaction Between Fluid and Vegetation Motion

In this analytical model, wave damping due to vegetation is described by the imaginary wave number k_i as expressed in (9). The linearized damping coefficient D governs the magnitude of k_i through the term ϵ in (19). On the other hand, the motion of vegetation is determined by (21) if the fluid velocity u_2 of the waves is known. The interaction effect between the wave and vegetation is expressed through the damping coefficient D which is iteratively calculated by (5) using the relative velocity u_r between the wave and vegetaion motion.

The height of the lower layer, d, is determined by the following approximate relation based on the length of vegetation, l_0, and the amplitude of ζ, denoted by $\hat{\zeta}$

$$d = \frac{l_0 + \sqrt{l_0^2 - \hat{\zeta}^2}}{2} \tag{23}$$

which implies that d decreases from $d = l_0$ as $\hat{\zeta}$ is increased from $\hat{\zeta} = 0$.

The calculation proceeds in the following order:

(i) Starting from the condition of no vegetation motion, for which $u_v = 0$ and $d = l_0$, the fluid velocity and complex wave number are calculated.

(ii) The motion of vegetation is then computed using (21) where the swaying velocity u_v is calculated at every vertical point over a whole wave period.

(iii) The damping coefficient D is determined by (5) using the relative velocity $u_r = (u - u_v)$.

(iv) The depth of the lower layer is calculated by (23).

(v) The fluid velocity and complex wave number are re-calculated using the obtained damping coefficient D.

(vi) The computation is repeated until the convergence of the solution is achieved.

(2) Calculated Results

The final expression of the vegetation motion given by (21) has many parameters. Although a sensitivity analysis on the wave dacay coefficient k_i and the wave celerity $c = \sigma/k_r$ may be made using the non-dimensional parameters, the variations of k_i and c are herein illustrated using the dimensional parameters whose ranges are related to the artificial seaweed experiment. In the following computations, use is made of $h = 27$cm, $l_0 = 25$cm, $N = 0.149 cm^{-2}$, $C_M = 2.0$, $b = 5.2$cm, $E = 9.8 * 10^7$g/(cm.sec^2), $I = bt^3/12$.
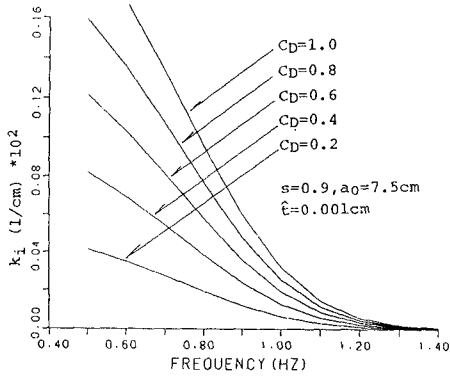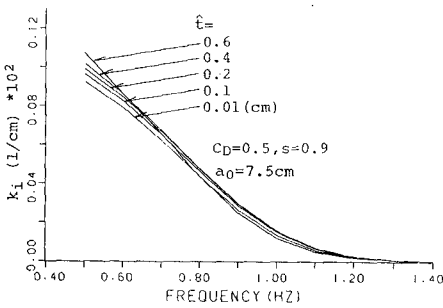
(a)
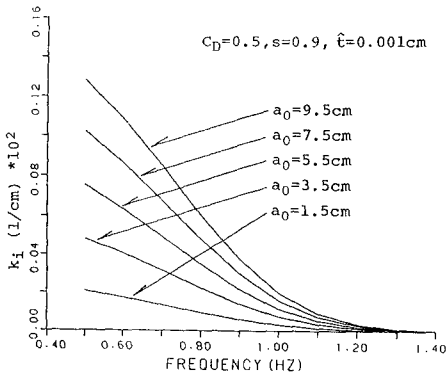
(b)

(c)

Figure 3: Computed wave dacay coefficient k_i
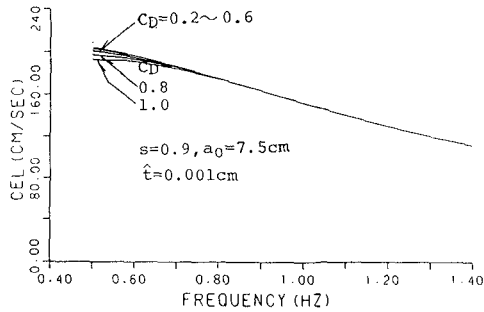
Figure 4: Computed wave celerity c

Fig. 3 (a),(b),(c) shows the variations of k_i with respect to the frequency $(\sigma/2\pi)$ for different values of C_D, a_0 and $\hat{t}$, respectively. The wave decay coefficient k_i increases with the drag coefficient C_D as well as with the wave amplitude a_0. The dependence of k_i on the wave amplitude results from the quadratic drag resistance used to estimate D in (5). Meanwhile, the increase of $\hat{t}$ results in the increase of the moment of inertia I, however, the stiffness of the vegetation material changes the wave decay coefficient very little. The change of the specific gravity s of the vegetation material, which modifies the restoring force by buoyancy, does not affect the decay coefficient much, although the computed results are not presented here.

On the other hand, the wave celerity c varies very little with the drag coefficient C_D as shown in Fig. 4. The other parameters a_0, $\hat{t}$, and s are also found to have negligible effects on c.

5. COMPARISON WITH EXPERIMENT
(1)Wave Damping Experiment by Using Artificial Seaweed

The extended model is compared with the artificial seaweed experiment conducted by Asano et al.(1988). The experiment was performed in a wave tank which was 27m long, 0.5m wide and 0.7m high as shown in Fig. 5. The model seaweed was made of polypropylene strips whose specific gravity was 0.9. The length, width and thickness of each strip was $l_0 = 25$cm, $b = 5.2$cm and $\hat{t} = 0.03$mm, respectively. Each strip was bound to a heavy wire netting such that the strip was normal to the side walls of the tank and could bend with little torsion under the action of monochromatic waves generated in the tank. The number of strips placed uniformly over the area of 4 m^2 was 4400 and 5960. Correspondingly, the number of strips per unit horizontal area was N=0.110 and 0.149 cm^{-2}. The water depth above the vertical strips was
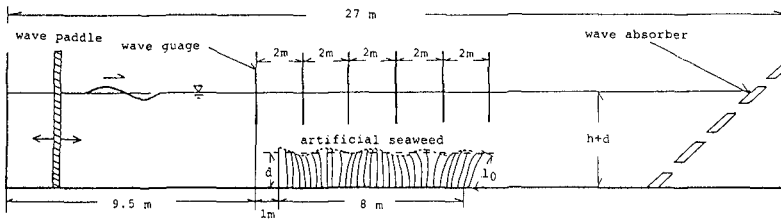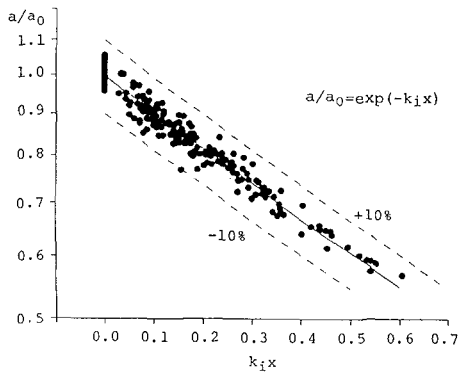
Figure 5: Experimental setup

Figure 6: Measured wave amplitudes fitted to exponential decay model

$h = 20$ and 27cm. In total, sixty test runs were performed.

Six capacitance wave gauges were used to measure the free surface oscil-
lations. Excluding the data from the two gauges at both ends, the data from
the remaining four gauges were used in the data analysis because this wave
damping model does not account for the presence of lateral boundaries. The
location of the second gauge in Fig.5 was taken herein to be the location x=0
and the analysis domain was $0 \leq x \leq 6$ m.

A regression analysis based on the method of least squares was performed
using (9) in which the exponential decay of the local wave amplitude a is
characterized by the initial amplitude a_0 at $x = 0$ and the exponential decay
coefficient k_i. Fig. 6 shows the measured values of a at x=0, 2, 4 and 6m for
the 60 runs, normalized as a/a_0 as a function of $k_i x$ where the fitted values
of a_0 and k_i are used for each run.

(2) RESULTS AND DISCUSSION

The comparisons on the decay coefficient k_i are shown in Fig. 7, where the circles indicate the measured values. The experimental results are shown separately for the large wave runs ($a_0 = 4.5 \sim 6.0$cm) and for the small wave runs ($a_0 = 2.8 \sim 4.2$cm), while the computed results are based on the average wave amplitude; $a_0=5.25$cm for the former and $a_0=3.50$cm for the latter.

The previous model of Kobayashi et al.(1992) reproduced the measured wave decay coefficients only when the drag coefficient C_D of the order 0.1 was used for the swaying vegetation. The present model including the swaying motion of the vegetation is shown to yield much better agreement with the same data set, using a more realistic value of the drag coefficient of approximately 0.5.

Fig. 8 shows the comparison between the measured and calculated values of the wave celerity c. Slight overestimation of c by the present model is apparent for low frequency waves. The agreement with the measured celerity becomes slightly worse when the swaying motion of vegetation is considered.

Besides the wave damping measurements, the horizontal displacements of the top of the vegetation strip under waves were measured. Fig. 9 shows the measured data points in comparison with the computed curves. As the wave frequency f decreases, the present model tends to overpredict the displacement ζ.

Judging from Figs. 8 and 9, the limitations of the present model seems to arise when the swaying motion becomes large. It was observed for low frequency waves that the vegetation swayed considerably and may have generated turbulence along the interface and among the vegetation strips. The present model,however, does not account for the turbulent stress. The modeling of the swaying vegetation is so simple that the complex large swaying motion could not be reproduced very accurately. The drag resistance of the vegetation may no longer be expressible by (3) which neglects the vertical component of the drag resistance.

Although the drag coefficient C_D is herein taken to be 0.5 as the best value for the measured decay coefficients, C_D should be a function of Reynolds number defined by the relative velocity and vegetation size. In addition, the proximity effects of surrounding strips on C_D should be examined because natural vegetation usually grows densely as a colony.

6. CONCLUSIONS

The present paper has presented an analytical solution for water waves propagating over submerged vegetation and a mathematical expression for
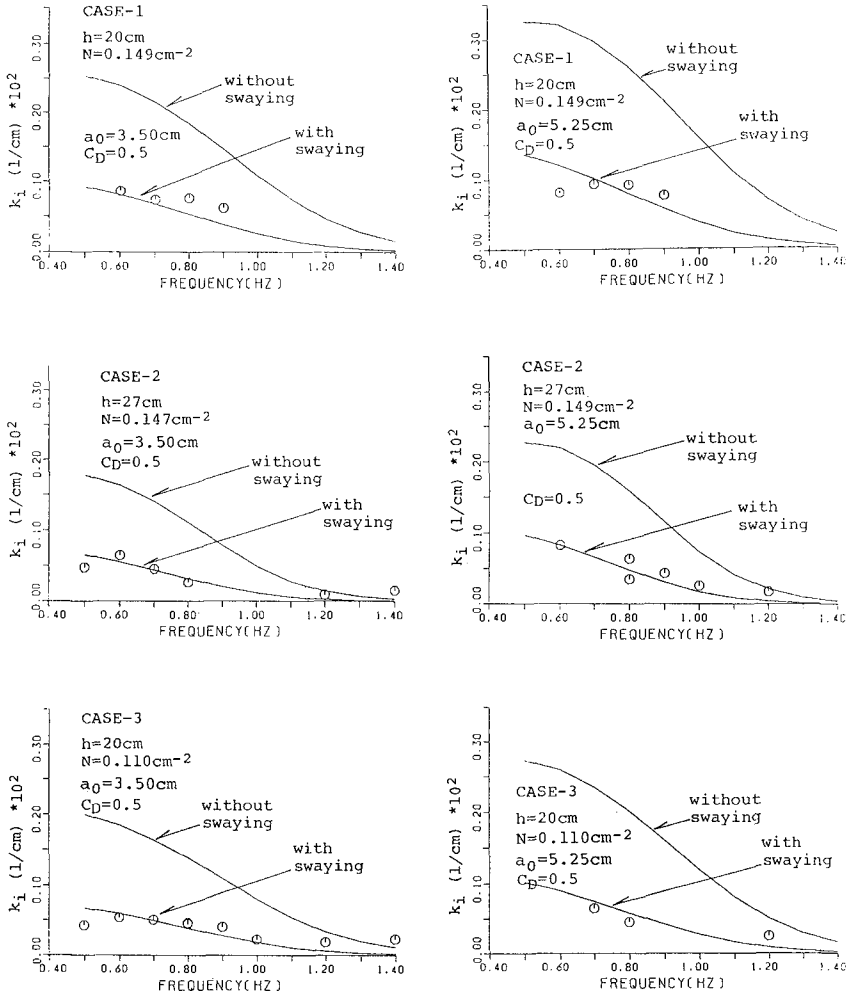
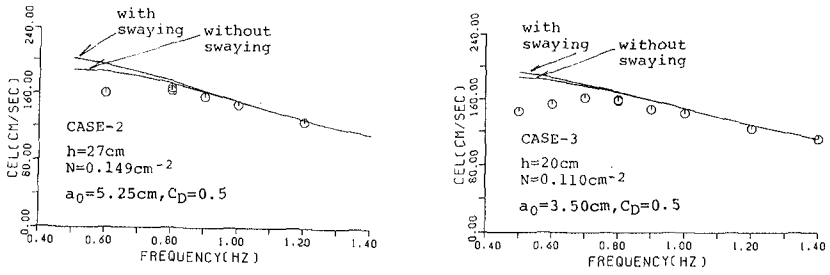Figure 7: Comparisons between measured and computed decay coefficient k_i

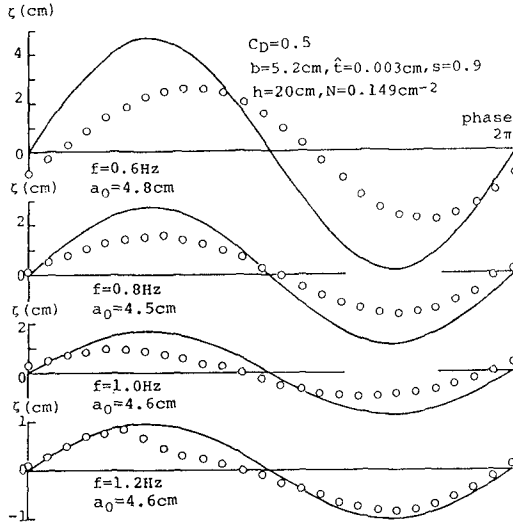Figure 8: Comparisons between measured and computed wave celerity c

Figure 9: Comparisons between measured and computed horizontal displacement of top of vegetation strip

vegetation motion swayed by the water waves. Both solutions have been linked by the linearized damping coefficient D through which the interaction effects between the water waves and vegetation motion have been accounted for. The properties of the wave decay coefficient and wave celerity have been examined by performing a sensitivity analysis.

The present model has been compared with the artificial seaweed experiment. The drag coefficient C_D has been calibrated using the exponential decay coefficient fitted for each run. The calibrated values have been found to be approximately 0.5 which is greater than the values of the order 0.1 obtained by the previous model which neglected the vegetation motion. The drag coefficient of about 0.5 appears to be more realistic. Although the present model is valid only when the swaying motion is not large, the capability for predicting the wave decay has been improved herein by including the vegetation motion in the model.

REFERENCES

Asano T., S. Tsutsui and T. Sakai (1988): Wave damping characteristics due to seaweed, Proc. 35th Coast. Engrg. Conf. in Japan, 138-142(in Japanese).

ASCE Task Committee on sea level rise and its effects on bays and estuaries (1992): Effects of sea level rise on bays and estuaries, J. Hydraulic Engrg., ASCE, 118(1), 1-10.

Jackson, G.A. (1984): Internal wave attenuation by coastal kelp stands, J. of Physical Oceanography, 14, 1300-1306.

Jenkins, S. A. and D. W. Skelly(1987): Hydrodynamics of artificial seaweed for shoreline protection, Scripps Inst. Oceano., SIO Ref. Ser., No. 87-16, p.66.

Kobayashi, N., A. W. Raichle and T. Asano(1992) : Wave attenuation by vegetation, J. of Waterway, Port, Coastal and Ocean Engineering, ASCE, 119(1), (in press).

Rogers, S. (1986): Artificial seaweed for shoreline erosion control, UNC Sea Grant Pub., UNC-SG-WP-8-6-4, Univ. of North Carolina, p.15.